

V CIRP Conference on Biomanufacturing

Mechanical and microstructural evaluation of solid-state foamed Ti6Al4V-ELI alloy

P. Guglielmi^a, A. Piccininni^a, A. Cusanno^a, A. A. Kaya^b, G. Palumbo^{a,*}

^aDMMM, Politecnico di Bari, Via Orabona 4, 70126 Bari Italy

^bMugla Sıtkı Kocman University, Engineering Faculty, Metallurgy and Materials Eng. Dept.

* Corresponding author. Tel.: +39 080 596 3719. E-mail address: Gianfranco.palumbo@poliba.it

Abstract

Metallic materials adopted in biomedical applications play a key role in the replacement of so-called "hard tissues" (the human bone). Titanium (Ti) alloy prostheses are considered the best among all metallic implants due to their mechanical performance, corrosion resistance and biocompatibility. In particular, Ti foams are characterized by properties very similar to those of human bone since the typical cell structure obtained by a foaming process is very similar to the microstructure of a trabecular bone. Therefore, foaming processes allow for obtaining less stiff prostheses than those composed of a bulk material, leading to reduced stress shielding.

In this work, strictly related to the national project FabriCARE, Ti-6Al-4V-ELI foam-based structures were investigated. Unlike those made of other alloys, Ti foams cannot be obtained directly from the liquid phase due to the excessive reactivity of this material with the environment. Thus, a Ti-based foam structure can be more conveniently produced by the solid-state process, which also allows to conveniently set the specific level of porosity, thus customizing the implant even from this point of view.

Ti powders were processed via Hot Isostatic Pressing (HIP) to obtain billets. Samples were then extracted via EDM from the billets, and then subjected to foaming process at different temperatures exploiting the physical simulator Gleeble system 3180. Foamed samples were properly prepared and subjected to microstructural and mechanical investigations to investigate the level of porosity and their dimensions along with the changes in mechanical properties.

© 2022 The Authors. Published by Elsevier B.V.

This is an open access article under the CC BY-NC-ND license (<https://creativecommons.org/licenses/by-nc-nd/4.0>)

Peer-review under responsibility of the scientific committee of the V CIRP Conference on Biomanufacturing

Keywords: Ti6Al4V-ELI, Metallic foams, Hot isostatic pressing, Microstructure, Mechanical properties

1. Introduction

Metallic materials, in addition to being among the first materials to be used for biomedical applications, are essential in the replacement of the so-called "hard tissues" such as human bone. Prosthetic implants in Ti alloy are considered among the best of all metal alloys. Furthermore, these alloys in the foamy form are characterized by properties very similar to those of human bone and able to appropriately withstand the loads to which they may be subjected; in fact, the typical cell structure is easily attributable to that of a trabecular bone. In addition, these properties allow: (i) to obtain less rigid prosthetic

implants than those conventionally obtained through the adoption of massive materials; (ii) to reduce stress shielding problems; (iii) to promote the regrowth of surrounding bones, when the open pore structure is positioned at the interface. In this regard, in recent years, implants such as porous Ti alloy scaffolds have motivated great interest due to the lower elastic modulus, associated with a greater propensity for bone regrowth [1,2]. Furthermore, Ti alloys are characterized by excellent properties such as (i) high mechanical strength, (ii) good corrosion resistance, (iii) biocompatibility and (iv) osteoconductivity [3-7].

It has been established that bone tissues are capable of remodeling due to applied loading [8]. The absence, or the

simple reduction of these loads, can cause bone loss [9]. Considering this aspect, the presence of very rigid parts drastically hinders the ability of the bone to respond to that same load; as anticipated, in these cases we speak of stress shielding.

One of the greatest advantages due to the use of metal foams is connected to the possibility of being able to vary (depending on the volume of the pores, the fraction and the dimensional distribution) the modulus of elasticity, bringing it as close as possible to that of the bone, significantly reducing the shielding phenomena. This aspect is confirmed by a significant increase in the in-vivo duration of prosthetic implants in porous titanium [10].

The size of the porosities and their typology, although there are no univocally recognized values as optimal, are mandatory for an improvement of the entire structure [11].

There are several methodologies capable of guaranteeing porous structures: (i) Space-holder, (ii) Replication, (iii) Generation of bubbles (controlled expansion of Argon, foaming in molten Ti and gel casting), (iv) Freeze casting and (v) Rapid prototyping.

These techniques have been widely successful from a commercial point of view in the manufacture of, for example, aluminum and zinc foams, but are not always optimal for Ti alloys. In this case, the solid-state foaming methodologies, on the other hand, can be considered as the most promising ones for obtaining porous structures.

High pressure Argon bubbles are created in a metal matrix by Hot Isostatic Pressing (HIP) of metal powders in the presence of Argon gas. The resulting material is characterized by a low fraction of pores (typically less than 1%) composed of numerous high-pressure Argon pores with dimensions of the order of microns. During subsequent heat treatment at elevated temperatures, the high-pressure gas allows the bubbles to expand by exploiting the slow creep of the surrounding metal material. According to different studies, following these heat treatments at very high temperatures (about 1250 °C) and of long duration, average increases in porosity of about 50% are recorded [13-15].

Among others, Oppenheimer and Dunand [16], with reference to the foaming process of a HIPed Ti-6Al-4V alloy, the expansion of the single pore during a cyclic heat treatment (conducted between 840 and 1030°C) improves both the foaming speed (reducing the flow tension) and the final porosity (delaying the fracture of the pores and the subsequent escape of the gas), compared to the isothermal expansion of the pores at 1030 °C, where creep is recognized as the only mechanism of control of the foaming process.

Increasing the Argon content in the billet increases the foaming rates for both creep and superplastic conditions. In the Ti-6Al-4V alloy, through the superplastic forming process it was possible to obtain a porosity value of approximately 52%, showing an optimal combination of strength (170 MPa) and stiffness (18 GPa) properties, which are very important aspects to manufacture prosthetic implants.

In the present work, some results of the national project FabriCARE are presented. In particular, the results obtained from the characterization in isothermal conditions (1020°C) and for different durations are discussed. Furthermore, through the proposed experimental methodology, the different foaming conditions were correlated to the mechanical properties (micro-hardness) through an analytical model subsequently validated.

2. Material and methodology

2.1. Investigated material

The experimental activity in this work was conducted using a titanium billet produced by Hot Isostatic Pressing (HIP): the manufacturing process of the billet was characterized by (i) Argon pressure of 0.2 MPa and (ii) HIP pressure equal to 80MPa. Ti6Al4V-ELI powders with a maximum diameter of 50µm were used.

The chemical composition of the investigated material is reported in Table 1.

Table 1. Chemical composition of the investigated Ti alloys.

Al%	V%	Fe%	C%	N%	H%	O%	Ti
5.88	3.87	0.14	0.22	0.006	0.002	0.112	Bal.

For the experimental activity, "Dog Bone" samples (thickness of 3mm) were extracted from the billet produced via HIP using an Electrical Discharge Machine, EDM. The main dimensions of the sample are shown in Fig. 1.

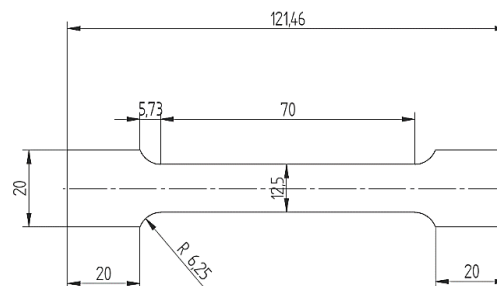


Fig. 1. Dimensions [mm] of the dog-bone sample adopted for the foaming tests.

2.2. Adopted methodology

The whole methodology proposed is schematized in the flowchart in Fig. 2.

The methodology can be divided in four different steps. Starting from the experimental foaming tests (Step 1) for which the architecture of a physical simulator was exploited to evaluate the effects of a wide range of temperatures with a single sample, microstructural investigations were conducted (Step 2) on different sections extracted from the samples obtained via EDM.

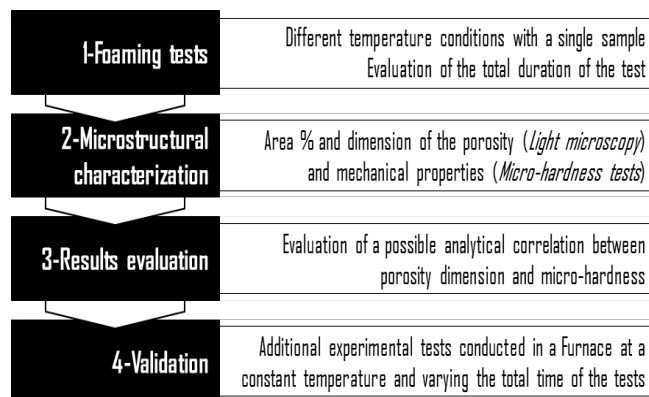


Fig. 2. Schematic overview of the proposed methodology.

The results thus obtained were processed to determine a correlation (Step 3) between the main dimensions of the porosities and the mechanical properties. Finally, the proposed approach was validated by means of further tests performed at a constant temperature by means of a furnace (Step 4).

2.3. Experimental foaming tests

Foaming tests were performed using the physical simulator Gleeble System 3180 capable of reproducing several technological conditions in high vacuum conditions and at high heating rates. During tests, the sample was heated by Joule effect (once the high vacuum condition was reached inside the test chamber) managing a PID controller to reach and maintain the temperature measured by a thermocouple welded in the middle area of the sample (TC1 in Fig 3). In addition, during the test, the sample was clamped between two grips cooled and kept at room temperature. The sample was thus characterized by a thermal gradient which determined a parabolic temperature distribution having its maximum value in the center. Taking advantage of this system architecture, during the experimental test, the samples were instrumented by means of four thermocouples (TCs) positioned as shown in Fig. 2.

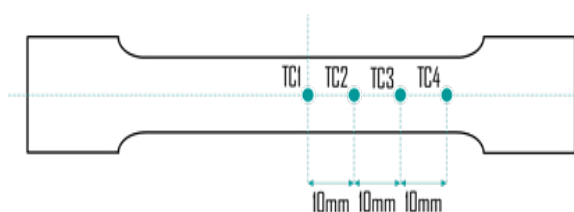


Fig. 3. Positioning of the thermocouples for the temperature acquisition.

While TC2 guaranteed the maximum temperature in the test, the other three thermocouples allowed to acquire the values at different positions from the center, thus subjected to different temperatures. In this way it was possible to acquire a lot of information by means of a single test, since it was possible to investigate a wide range of temperatures and their effect on the material in terms of foaming.

The experimental campaign was based on 4 different test durations (60, 120, 180 and 240 minutes) maintaining a constant temperature of 1020°C in the center of the sample.

2.4. Metallographic analyses

In order to evaluate the level of porosity according to the investigated foaming conditions, 6 different cross sections with a 5mm step (starting from the center to the peripheral area of the sample) were extracted, mounted, grinded and polished. In fact, an appropriate metallographic preparation was required for both the observation with the light microscope and the microstructural characterization by means of Vickers microhardness tests.

Specifically, the microscopic investigation aimed at determining both the average diameter and the percentage area of the porosities according to the different temperatures and durations. For this purpose, the Nikon MA200 microscope and the ImageJ software for digital image processing were used.

2.5. Microhardness tests

To characterize the foamed material from a mechanical point of view, 10 different Vickers microhardness measurements were performed using an automatic Qness Q10 Microhardness tester and setting a load of 500g. In addition, results coming from the two different approaches were processed to evaluate a possible analytical correlation.

2.6. Experimental validation of the proposed methodology

Finally, to validate the proposed methodology, further tests were conducted in a Nabertherm Furnace at a constant temperature and setting different durations.

3. Results and Discussion

3.1. Experimental foaming tests

Some images concerning the experimental phase are shown in Fig. 3: It is possible to observe the effect of the volumetric growth of the sample during (Fig. 3a) and after (Fig. 3b) the foaming test.

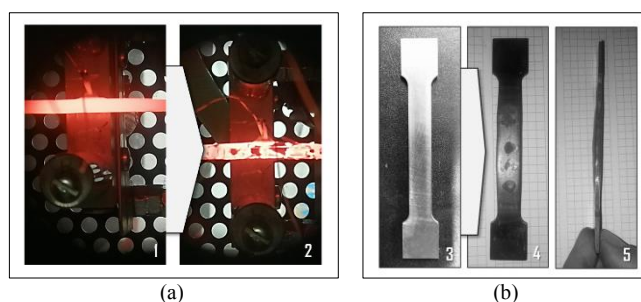


Fig. 4. (a) Experimental test at the beginning (1) and at the end (2); (b) "Dog Bone" sample before (3) and after (4, 5) the foaming test.

Regarding the foaming tests, the temperature distribution obtained along the longitudinal direction is shown in the graph in Fig. 5.

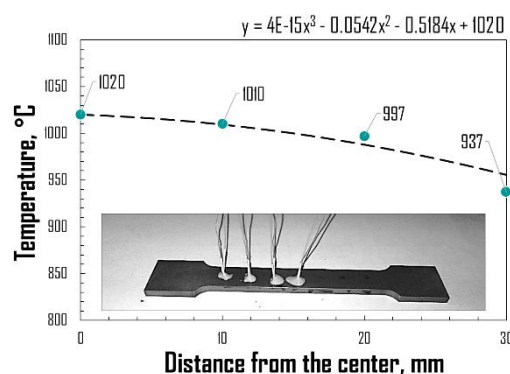


Fig. 5. Temperature distribution along the longitudinal direction.

The green markers indicate the experimental measurements acquired by the four thermocouples welded to the sample, while the black dashed line represents the three-degree polynomial curve fitting experimental data.

Thanks to this approximation it was possible to associate a temperature value at different positions along the sample: Table 2 shows the temperature levels experienced by the

material at each position where the sections considered for the metallographic analysis were extracted.

Table 2. Estimated temperature at different longitudinal position.

Longitudinal position, mm	Estimated temperature, °C
0	1020
5	1016
10	1009
15	1000
20	988
25	973

3.2. Metallographic analyses

Fig. 6 shows the micrographs of different sections of the same sample heat treated at a constant temperature of 1020°C for 240 minutes. It is possible to evaluate the effect of the thermal gradient along the longitudinal direction of the sample (in accordance with the temperature value reported in Table 2).

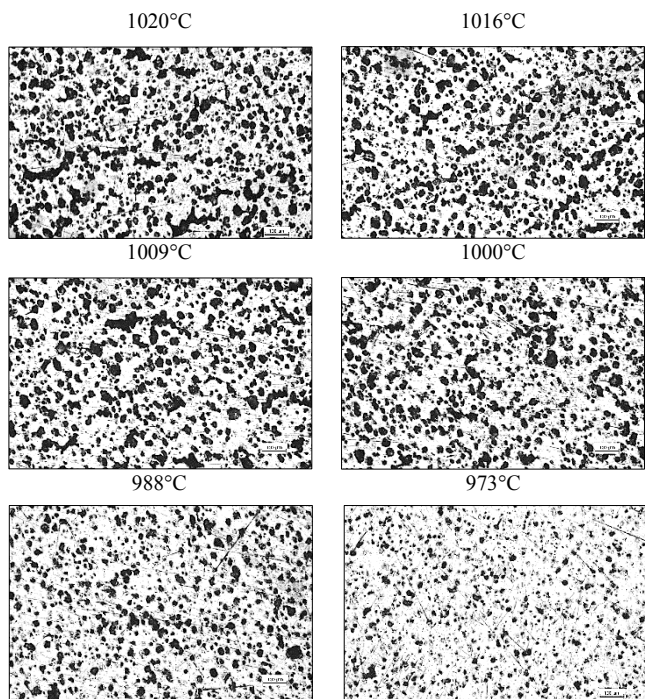


Fig. 6. Temperature effect in the longitudinal direction for a single test performed for 240 minutes.

Even small variations in temperature determined different size and percentages of the pores. This is evident if the two extreme sections (corresponding to a temperature of 1020°C, in the center of the sample, and 973°C, 25mm away from the center of the sample) are considered. The previous observations can be extended to all investigated conditions: in fact, as shown in the graphs in Fig. 7 and in Fig. 8, in particular for the longest durations, the amount of porosity and the size of the pores increased according to the temperature level (this is more evident in the trends shown in fig. 7, thus in terms of average size of the pores).

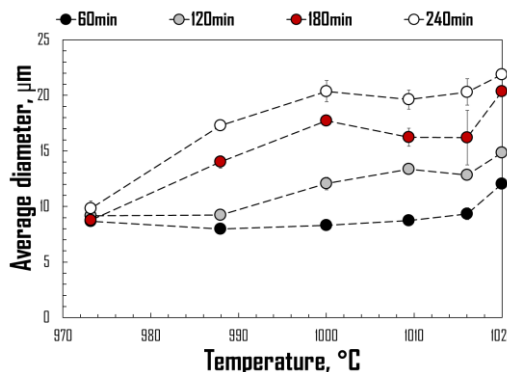


Fig. 7. Effect of temperature in terms of average diameter of the porosity.

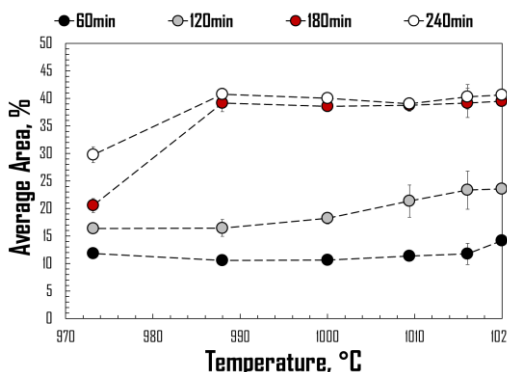


Fig. 8. Effect of temperature in terms of average area of the porosity.

Specifically, keeping constant the temperature at 1020°C and varying the foaming time from 60 to 240 minutes, the size of the pores showed an increase equal to about 45% (from 12 microns after 60 minutes to 21.9 microns after 240 minutes). Moreover, considering the same duration of the heat treatment (i.e., 240 minutes), an increase of the pores size of about 55% was obtained by increasing the temperature from 973 to 1020°C. In addition to the effect of the temperature on the foaming kinetics, as reported in Fig. 9, also the observation of the micrographs referred to the central section (the one constantly at 1020°C) for the 4 investigated test durations showed a strong influence in terms of foaming capability of the investigated HIPed Ti alloy.

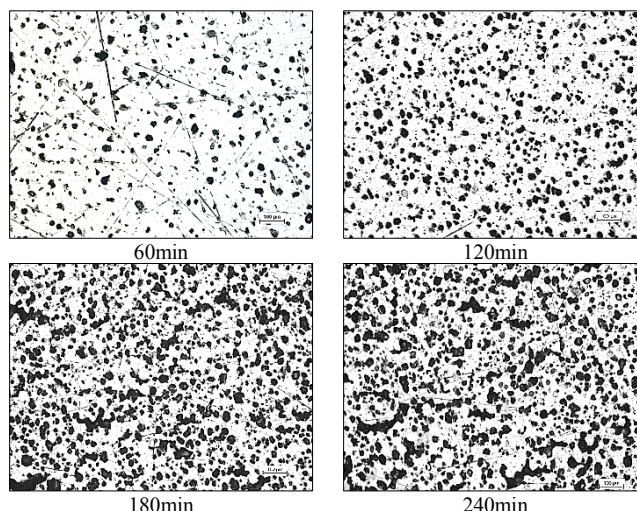


Fig. 9. Effect of the duration of the test at a fixed temperature of 1020°C.

3.3. Microhardness tests

Considering the same samples and sections analyzed with the light microscope, the micro-hardness tests allowed to evaluate the effect of the foaming phenomenon on the mechanical properties of the alloy. An example of the influence of the porosity level on the corresponding hardness value is shown in the two micrographs in Fig. 10. In fact, it is possible to observe how the dimple due to the indenter is much larger in correspondence with a greater size and percentage of porosities.

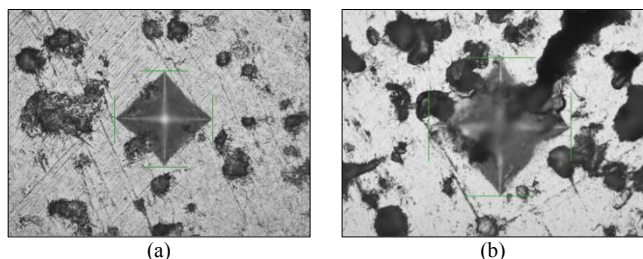


Fig. 10. Micro-hardness tests in correspondence of both low (a) and high (b) porosity levels.

Results coming from the experimental micro-hardness tests confirmed the trend obtained by means of the metallographic analysis.

As shown in the graph in Fig. 11, as the temperature increased the mechanical properties decreased; similarly, considering a fixed value of temperature, the duration of the forming determined the same effect.

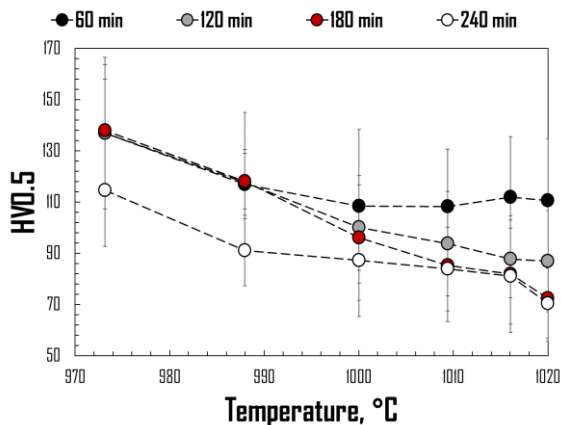


Fig. 11. Micro-hardness trends according to the different values of the temperature and foaming duration.

Considering a heat treatment duration equal to 240 minutes, as the temperature varied from a minimum value of 973°C to a maximum value of 1020°C, the micro-hardness value decreased from 114.61 HV0.5 to 70.48 HV0.5 respectively with an overall decrease of 39%. In addition, at a fixed temperature value (1020°C) an increase in terms of the test duration from 60 to 240 minutes determined a reduction of the average microhardness value of about 36% (from 110.56 to 70.48 HV0.5).

According to the consistency of the results obtained in terms of both porosity and micro-hardness values, as shown in Fig. 12, it is possible to observe a good correlation between the two different outputs; in particular, such a correlation was

expressed using a second order polynomial fitting.

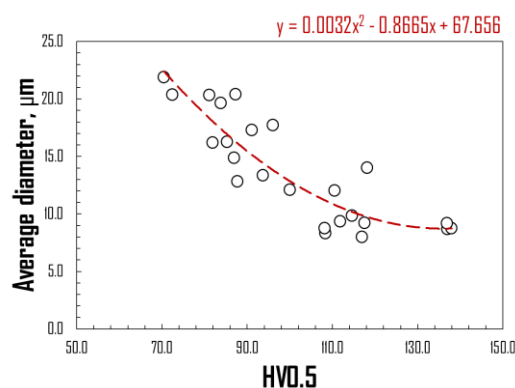


Fig. 12. Correlation between the average diameter of porosity and hardness values recorded.

3.4. Experimental validation of the proposed methodology

The result obtained shows a potential tool capable of predicting the level of porosity as a function of micro-hardness value and vice versa, regardless of the time-temperature couple characterizing the foaming process.

At this point, the final step of the proposed methodology is represented by the validation of the analytical trend through additional experiments conducted in furnace at a constant temperature of 973°C (the minimum investigated through the tests carried out with the physical simulator) and for all different durations previously tested.

Once again, the micrographs in Fig. 12 showed an increase, even if not marked, in terms of average pore size as the foaming times increased.

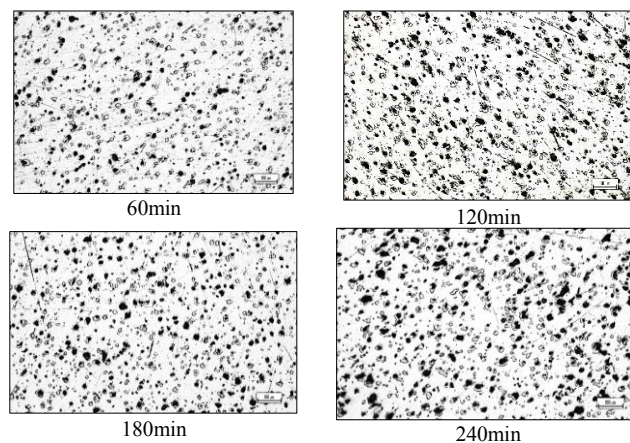


Fig. 13. Time effect at a fixed temperature of 973°C.

Table 3 shows the hardness and the average diameter values of the porosities experimentally determined.

Table 3. Experimental results referred to the tests on furnace at 973°C.

Total time, min	HV0.5	Porosity diameter
60	139.7±11.0	8.66
120	135.6±17.9	9.76
180	132.2±15.3	10.02
240	108.7±15.3	12.10

In addition, according to the previous results in terms of micro-hardness values and considering the analytical model using for correlating experimental data, it was possible to predict the value of the average diameter of the porosity (Table 4).

Table 4. Experimental vs analytical diameter of the porosity.

Time, min	Experimental diameter	Analytical diameter
60	8.66	9.03
120	9.76	9.00
180	10.02	9.06
240	12.10	11.28

The capability of the analytical law to predict the value of the average diameter of the pores was evaluated by means of the Root Mean Square Deviation (RMSD), as expressed by Equation 1:

$$RMSD = \sqrt{\frac{\sum_{i=1}^N \|x_e - x_a\|^2}{N}} \quad (1)$$

being N the total number of acquired experimental data and x_e and x_a the experimental and the analytical values of the porosity diameter, respectively.

The results obtained supported the goodness of the proposed methodology since the RMSD value is equal to 0.76.

4. Conclusions

In the present work a methodology aimed to determine in a fast way the porosity level due to the foaming process at constant temperature on a HIPed Ti alloy was proposed. In this regard, the adoption of the Gleeble system 3180 physical simulator proved to be effective.

The capability of the investigated HIPed Ti alloy to foam was directly correlated to both the test temperature and its duration. In particular, when the foaming test duration was set to 240 minutes, an increase of the temperature from 973 to 1020°C determined an increase of the average pore size of about 55%. At the same time, considering a foaming temperature of 1020°C, expanding the duration from 60 to 240

minutes determined an increase of the porosity approximately equal to 45%.

An inverse trend was associated to the micro-hardness values: the values decrease up to 39% with an increase in temperature (from 973 to 1020°C) at a fixed duration (240 minutes) and up to 36% with an increase in the duration of the heat treatment (from 60 to 240 minutes) at 1020°C.

Furthermore, the analyses carried out allowed to correlate the porosity and the micro-hardness values using a second-order polynomial model.

The analytical relationship was successfully validated through additional foaming tests carried out at constant and uniform temperature while setting the same durations of the tests previously conducted.

References

- [1] D. W. Hutmacher: *Biomaterials*, 2000, 21, (24), 2529–2543.
- [2] R. Langer and J. P. Vacanti: *Science*, 1993, 260, (5110), 920–926
- [3] D. C. Dunand: *Adv. Eng. Mater.*, 2004, 6, (6), 369–376.
- [4] C. E. Wen: *J. Mater. Sci. Mater. Med.*, 2002, 13, (4), 397–401.
- [5] C. E. Wen, M. Mabuchi, Y. Yamada, K. Shimojima, Y. Chino and T. Asahina: *Scr. Mater.*, 2001, 45, (10), 1147–1153.
- [6] M. Bram, H. P. Buchkremer, A. Laptev and D. Stover: *Proc. Int. Conf. on 'Cellular metals and metal foaming technology'* Bremen, MIT-Verlag, 2001, 215–220,
- [7] M. Bram, C. Stiller, H. Buchkremer, D. Stover and H. Baur: *Adv. Eng. Mater.*, 2000, 2, (4), 196–199
- [8] L. J. Gibson and M. F. Ashby: 'Cellular solids-structure and properties'; 1997, Cambridge, Cambridge University Press
- [9] G. H. van Lenthe, M. C. de Waal Malefijt and R. Huiskes: *J. Bone Joint Surg. Br.*, 1997, 79-B, (1), 117–122
- [10] S. J. Hollister: *Nat. Mater.*, 2005, 4, (7), 518–524
- [11] R. Singh, P. D. Lee, R. J. Dashwood and T. C. Lindley, *Mater. Technol.*, 2010, 25
- [12] M.W. Kearns, P.A. Blenkinsop, A.C. Barber, and T.W. Farthing, *Met. Mater.* 3(2), 85 (1987)
- [13] M.W. Kearns, Formation of Porous Bodies U.S. Patent (IMI Titanium Limited, 1987), U.S. Patent No. 4 659 545
- [14] M.W. Kearns, P.A. Blenkinsop, A.C. Barber, and T.W. Farthing, *Int. J. Powder Metall.*, 1988 24(1), 59
- [15] R.L. Martin, Integral Porous-Core Metal Bodies and in situ Methods of Manufacture Thereof U.S. Patent (McDonnell Douglas Corp., 1996), U.S. Patent No. 5 564 064.
- [16] Scott Oppenheimer, David C. Dunand, *J. Mater. Res.*, Vol. 16, No. 5, May 2001